

**Band alignments and polarization properties of the Zn-IV-nitrides**

Journal:	<i>Journal of Materials Chemistry C</i>
Manuscript ID	TC-ART-03-2020-001578.R1
Article Type:	Paper
Date Submitted by the Author:	04-May-2020
Complete List of Authors:	Adamski, Nicholas; University of California Santa Barbara, Electrical and Computer Engineering Wickramaratne, Darshana; University of California Santa Barbara, Materials Department; US Naval Research Laboratory, Center for Computational Materials Science Van de Walle, Chris; University of California Santa Barbara, Materials Department

Cite this: DOI: 00.0000/xxxxxxxxxx

## Band alignments and polarization properties of the Zn-IV-nitrides

Nicholas L. Adamski,<sup>\*a</sup> Darshana Wickramaratne,<sup>b,c</sup> and Chris G. Van de Walle<sup>d</sup>

Received Date

Accepted Date

DOI: 00.0000/xxxxxxxxxx

Zn-IV-nitrides have a range of potential applications in electronic and optoelectronic devices and can be integrated with currently used III-nitride semiconductors and their alloys. Using hybrid density functional theory, we examine band gaps, band offsets and polarization properties of the Zn-IV-nitrides and the ramifications of these properties on heterointerfaces formed between the Zn-IV-nitrides and III-nitrides. We find a type-II band alignment between ZnGeN<sub>2</sub> and GaN, where the valence band of GaN is 0.28 eV above the valence band of ZnGeN<sub>2</sub>. Heterostructures between Zn-IV-nitrides and III-nitrides result in interface charges that allow for novel heterostructures and increased control over polarization fields. We find that an interface between In<sub>x</sub>Ga<sub>1-x</sub>N and ZnGeN<sub>2</sub> can lead to zero interfacial polarization charge; however, the band alignments are unfavorable for carrier confinement in light-emitting devices. At the interface between AlN and ZnSiN<sub>2</sub>, we predict a large two-dimensional electron gas to form, confined to the ZnSiN<sub>2</sub> layer.

## 1 Introduction

The Zn-IV-nitrides have a wide range of band gaps, from 1.4 eV for ZnSnN<sub>2</sub> to 4.8 eV for ZnSiN<sub>2</sub>, rendering them promising for a variety of electronic and photonic devices.<sup>1,2</sup> The Zn-IV-nitrides, like the wurtzite (wz) III-nitrides, exhibit spontaneous polarization and piezoelectric effects.<sup>3,4</sup> The polarization leads to large bound charges at the interface, which can either be a detriment or provide useful functionality for device operation.

Taking advantage of the small lattice mismatch between Zn-IV-nitrides and the III-nitrides, a variety of device applications have been proposed based on heterostructures involving both sets of materials.<sup>5-7</sup> Simulations for light-emitting devices using InGaN-ZnGeN<sub>2</sub> type-II quantum wells have been reported.<sup>6,7</sup> The success of these designs depends on large band offsets between InGaN and ZnGeN<sub>2</sub> that realign the electron and hole wavefunctions and increase recombination. Accurate knowledge of the conduction- and valence-band offsets at heterojunctions between Zn-IV-nitrides and III-nitrides is therefore essential.

Polarization-matched quantum wells<sup>8</sup> is another application where Zn-IV-nitrides may be useful. In light-emitting devices polarization discontinuities produce a Stark effect that reduces efficiency.<sup>9</sup> On the other hand, large polarization discontinuities can be favorable for electronic devices since they lead to high-

density two-dimensional carrier gases at interfaces.<sup>10</sup> Interest in controlling these polarization charges has led to the field of polarization engineering,<sup>11</sup> which relies on the manipulation and control of ternary and quaternary alloy concentrations to identify polarization differences that are beneficial for the intended device application, taking lattice-matching constraints into account.

The structure of the Zn-IV-nitrides (ZnSnN<sub>2</sub>, ZnGeN<sub>2</sub>, and ZnSiN<sub>2</sub>) can be envisioned as starting from (e.g.) GaN in the wz structure and replacing pairs of Ga atoms with Zn-(group-IV) pairs. While this lowers the symmetry (the Zn-IV-nitrides have an orthorhombic structure with a 16-atom unit cell), we can still expect the Zn-IV-nitrides to display electronic and polarization properties similar to the wz III-nitrides. In Fig. 1(a,b), we illustrate the structure of GaN and ZnGeN<sub>2</sub>. The lattice parameters of ZnGeN<sub>2</sub> can be related to those of GaN by the relations:  $a \approx \sqrt{3}a_{wz}$ ,  $b \approx 2a_{wz}$ , and  $c \approx c_{wz}$ , where  $a_{wz}$  and  $c_{wz}$  are the wz lattice parameters.

A number of studies have addressed band alignments using density functional theory (DFT) based on explicit interface calculations in a superlattice geometry. Punya *et al.*<sup>12,13</sup> calculated the band alignments between ZnGeN<sub>2</sub>, ZnSnN<sub>2</sub>, GaN, and ZnO using the local density approximation (LDA) and a GW correction. They found a large valence-band offset of -1.4 eV at the ZnSnN<sub>2</sub>/GaN interface, and a valence-band offset of -1.1 eV at ZnGeN<sub>2</sub>/GaN, where the negative sign indicates that the valence-band maximum (VBM) of GaN is lower in each case. These results distinctly differ from those of Wang *et al.*,<sup>14</sup> who calculated offsets between ZnSnN<sub>2</sub>, GaN, and ZnO using the hybrid functional of Heyd, Scuseria and Ernzerhof (HSE)<sup>15,16</sup> and found a much smaller valence-band offset of -0.39 eV between ZnSnN<sub>2</sub> and GaN. Both Punya *et al.*<sup>12,13</sup> and Wang *et al.*<sup>14</sup> found that strain at

<sup>a</sup> Department of Electrical and Computer Engineering, University of California, Santa Barbara, CA 93106-9560, USA. E-mail: nadamski@ucsb.edu

<sup>b</sup> Materials Department, University of California, Santa Barbara, CA 93106-5050, USA.

<sup>c</sup> Center for Computational Materials Science, US Naval Research Laboratory, Washington, DC 20375, USA.

<sup>d</sup> Materials Department, University of California, Santa Barbara, CA 93106-5050, USA.

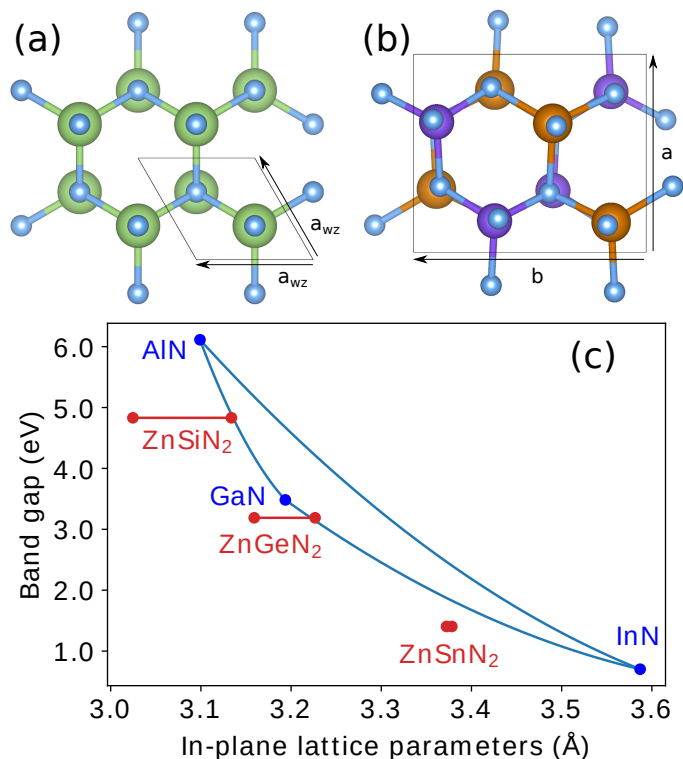


Fig. 1 (a) Wurtzite GaN and (b) orthorhombic ZnGeN<sub>2</sub> crystal structure viewed along the  $c$  axis. The respective primitive unit cells are shown with a black outline.  $a_{wz}$  is the in-plane lattice parameter for GaN, while  $a$  and  $b$  are the in-plane lattice parameters for ZnGeN<sub>2</sub>. (c) In-plane lattice parameters and band gaps for the Zn-IV-nitrides and III-nitrides. The two data points for the Zn-IV-nitride materials are the wurtzite-equivalent lattice parameters  $a/\sqrt{3}$  and  $b/2$ .

the interface affects the alignments by less than 0.1 eV. Recently, Cao *et al.*<sup>17</sup> calculated the offset between cubic GaN and cubic ZnGeN<sub>2</sub> with the HSE functional and found the valence-band offset for ZnGeN<sub>2</sub>/GaN to be  $-0.38$  eV, different by 0.7 eV from the results of Punya *et al.*<sup>12,13</sup> Experimentally, the valence- and conduction-band alignments for ZnSn<sub>1-x</sub>Ge<sub>x</sub>N<sub>2</sub> alloys of varying composition were measured using x-ray emission and absorption by Narang *et al.*,<sup>18</sup> who found the valence band of ZnGeN<sub>2</sub> to be slightly lower than that of ZnSnN<sub>2</sub>, and the conduction band of ZnGeN<sub>2</sub> to be significantly higher than that of ZnSnN<sub>2</sub>.

These inconsistencies (by up to 1 eV) between band alignments reported by different groups prompted us to re-examine band alignments using two different methodologies: (1) using surface calculations to align the electrostatic potential to the vacuum level,<sup>19</sup> and (2) using alignment based on the (+/-) level of interstitial hydrogen.<sup>20</sup> We apply both methods to determine the band alignments between the Zn-IV-nitrides and GaN, and compare the results to previous reports.

Some prior results on polarization properties of the Zn-IV-nitrides have also been reported. Paudel *et al.*<sup>4</sup> calculated stiffness tensors, spontaneous polarization, and piezoelectric coefficients. They reported spontaneous polarization values for ZnSnN<sub>2</sub>, ZnGeN<sub>2</sub>, and ZnSiN<sub>2</sub> between  $-0.022$  Cm<sup>-2</sup> and  $-0.029$  Cm<sup>-2</sup> and concluded that, since differences between

these values are markedly smaller than between III-N compounds, polarization-induced electric fields would be significantly suppressed at heterostructures between II-IV-nitrides. However, these spontaneous polarization values were calculated referenced to a zinc-blende (zb) structure. Recent work on wz nitrides has demonstrated that differences in spontaneous polarization values referenced to the zb structure require corrections to account for lattice-parameter differences.<sup>21</sup> Such corrections were not included in the work of Ref. 4. In the present work, we evaluate the spontaneous polarization values for the Zn-IV-nitrides using a proper centrosymmetric reference.<sup>21</sup> We also perform calculations of the proper piezoelectric constants and the stiffness tensors to generate a consistent set of parameters.

Our results allow us to determine the magnitude of polarization charges at Zn-IV-nitride/III-nitride heterostructure interfaces. Using these polarization properties, along with our calculated band alignments, we can identify interfaces with significantly reduced polarization charge, as well as interfaces with increased polarization charge that are favorable for applications in electronic devices.

## 2 Computational Methods

### 2.1 Density functional calculations

The calculations are performed using DFT with the hybrid functional of Heyd, Scuseria, and Ernzerhof (HSE),<sup>15,16</sup> as implemented in the Vienna *Ab initio* Simulation Package (VASP).<sup>22,23</sup> We use a plane-wave cutoff energy of 500 eV, and projector-augmented-wave potentials<sup>24</sup> with Zn  $3d^{10}4s^2$ , Ga  $4s^24p^1$ , Si  $3s^23p^2$ , Ge  $4s^24p^2$ , Sn  $5s^25p^2$ , and N  $2s^22p^3$  electrons in the valence. For GaN, we use a  $8 \times 8 \times 6$   $\Gamma$ -centered  $k$ -point grid, and adjust the HSE mixing parameter to reproduce the experimental band gap; at 29.5% we obtain a band gap of 3.48 eV. For the Zn-IV-nitrides, we use a  $4 \times 4 \times 4$  Monkhorst-Pack  $k$ -point grid. The band gaps of the Zn-IV-nitrides are not well established. We therefore use the default mixing parameter of 25%, which provides a good description of the physical and electrical properties. Our calculated lattice parameters and band gaps are included in Table 1; the lattice parameters are in good agreement with experimental values.<sup>1,25,26</sup> In Fig. 1(c) we show the in-plane lattice parameters and band gaps for the III-nitrides and Zn-IV-nitrides.

### 2.2 Band alignments

In order to determine band alignments, we first calculate the bulk electronic structure for each material. The eigenvalues that determine the band structure are referenced to the average electrostatic potential. In a bulk calculation, this average electrostatic potential is arbitrary (and commonly set to zero), and hence cannot serve to align different materials. We can align the bulk electrostatic potential to the vacuum level by performing a surface calculation, using a geometry in which a slab of material is surrounded by vacuum. By taking a macroscopic average,<sup>27</sup> we can compare the average electrostatic potential within the slab to the electrostatic potential in vacuum. We can then use this value to

Table 1 Calculated lattice parameters and band gaps for the Zn-IV-nitrides and GaN; experimental values are included for comparison. For AlN and InN, we use calculated values from Ref. 21

	Property	HSE	Expt.
ZnSnN <sub>2</sub>	<i>a</i> (Å)	5.85	5.84 <sup>†</sup>
	<i>b</i> (Å)	6.74	6.75 <sup>†</sup>
	<i>c</i> (Å)	5.47	5.46 <sup>†</sup>
	<i>E<sub>g</sub></i> (eV)	1.40	...
ZnGeN <sub>2</sub>	<i>a</i> (Å)	5.47	5.45 <sup>‡</sup>
	<i>b</i> (Å)	6.45	6.44 <sup>‡</sup>
	<i>c</i> (Å)	5.20	5.19 <sup>‡</sup>
	<i>E<sub>g</sub></i> (eV)	3.19	...
ZnSiN <sub>2</sub>	<i>a</i> (Å)	5.24	5.25 <sup>§</sup>
	<i>b</i> (Å)	6.27	6.28 <sup>§</sup>
	<i>c</i> (Å)	5.02	5.02 <sup>§</sup>
	<i>E<sub>g</sub></i> (eV)	4.83	...
InN ( $\alpha = 25\%$ )	<i>a</i> (Å)	3.59 <sup>¶</sup>	3.55 <sup>  </sup>
	<i>c</i> (Å)	5.76 <sup>¶</sup>	5.70 <sup>  </sup>
	<i>E<sub>g</sub></i> (eV)	0.65 <sup>¶</sup>	0.78 <sup>  </sup>
GaN ( $\alpha = 29.5\%$ )	<i>a</i> (Å)	3.19	3.19 <sup>  </sup>
	<i>c</i> (Å)	5.19	5.19 <sup>  </sup>
	<i>E<sub>g</sub></i> (eV)	3.48	3.51 <sup>  </sup>
AlN ( $\alpha = 31\%$ )	<i>a</i> (Å)	3.10 <sup>¶</sup>	3.11 <sup>  </sup>
	<i>c</i> (Å)	4.96 <sup>¶</sup>	4.98 <sup>  </sup>
	<i>E<sub>g</sub></i> (eV)	6.04 <sup>¶</sup>	6.25 <sup>  </sup>

align the bulk band structure to the vacuum level.

Nitride devices are usually grown along the *c* axis. However, performing band-alignment calculations for *c*-plane orientations is very challenging due to the presence of polarization fields. In slab calculations, the presence of dissimilar *+c* and *-c* interfaces complicates calculation of the offset; in addition, spurious fields will appear in the vacuum layer. Similar problems occur in superlattices calculations. Calculations for band alignments in the III-nitrides have conventionally been performed for nonpolar planes, and the resulting values have been successfully used for device modeling. Calculations for GaN were performed using slabs with nonpolar (1 $\bar{1}00$ ) (*m*-plane) surfaces. For the Zn-IV-nitrides we use (100) slabs which are also nonpolar and analogous to the *m* plane in III-nitrides. We use a  $8 \times 1 \times 1$  slab in a supercell geometry, separated by 20 Å of vacuum, and a  $1 \times 4 \times 4$  Monkhorst-Pack *k*-point grid.

Valence-band alignments are calculated based on the VBM in each material. To determine the band alignments between Zn-IV-nitrides and III-nitrides, we first determine alignments to GaN, then use the results of Moses *et al.*<sup>19</sup> to align to AlN and InN. Note that in Ref. 19 alignments were expressed for an average of the top three valence bands; we have combined those values with values of crystal-field splitting to obtain the VBM positions

reported in the present work.

An alternative way to calculate alignments between different materials is based on using the charge-state transition level of an interstitial hydrogen impurity (*H<sub>i</sub>*) as a common reference.<sup>20</sup> The (+/−) charge-state transition level for interstitial hydrogen, which we will label *H<sub>i</sub>*(+/−), is defined as the Fermi level (referenced to the VBM) at which *H<sub>i</sub>* has the same formation energy in the + and − charge states.<sup>29</sup> We calculate the formation energies of the *H<sub>i</sub>* impurity in a  $2 \times 2 \times 2$  supercell with 128 atoms and using a single special *k* point (1/4, 1/4, 1/4).<sup>29</sup> Spin polarization is included.

### 2.3 Polarization

Polarization properties are calculated using the modern theory of polarization<sup>30,31</sup> following Ref. 21. The electronic portion of the formal polarization is calculated by integrating the Berry phase over the Brillouin zone, while the ionic contribution is a sum over the coordinates of the nuclei in the unit cell. The formal polarization is a multivalued vector that is only defined modulo the quantum of polarization  $\frac{e\mathbf{R}}{\Omega}$ , where *e* is the electron charge, *R* is a lattice vector, and  $\Omega$  is the volume of the unit cell.<sup>32</sup> To calculate differences between materials, it is necessary to compare the appropriate branches of the polarization. This is typically done by computing the difference in formal polarization between the structure of interest and a high-symmetry reference structure and defining an effective spontaneous polarization. However, errors can arise if the formal polarization of the reference structure does not have a branch at zero. The commonly chosen zb reference has nonzero formal polarization that explicitly depends on the lattice parameters of the material; therefore, in considering spontaneous polarization differences between materials with different lattice parameters, a lattice-dependent correction should be included.<sup>21</sup> To avoid this extra step (which is commonly omitted in calculations for III-nitrides), it is preferable to instead choose a centrosymmetric reference structure that has a branch of the formal polarization at zero.

For the wz III-nitrides, the appropriate centrosymmetric structure is the layered hexagonal structure with space group *P6<sub>3</sub>/mmc*. In this structure, the group-III cations and the N anions are co-planar in the planes normal to the *c* axis. The formal polarization of the layered hexagonal structure has a branch at **0** and as such it serves as a suitable reference structure to define the effective spontaneous polarization for AlN, GaN, and InN.<sup>21</sup> An analog of the layered hexagonal structure can be constructed for the Zn-IV-nitrides. Starting from the orthorhombic ground-state structure (space group *Pna2<sub>1</sub>*), atoms are translated along the *c* axis to two planes normal to the *c* axis, such that group-II, group-IV, and N atoms are all situated within the same planes. This new structure is nonpolar, has a center of inversion symmetry, and has the space group *Pnma*. We will use this *Pnma* as the reference structure to calculate spontaneous polarization in the Zn-IV-nitrides, and we will call the resulting effective polarization *P<sub>sp</sub>*.

When the materials are strained, piezoelectric polarization will be present. In order to determine the proper piezoelectric con-

<sup>†</sup> Ref. 1

<sup>‡</sup> Ref. 25

<sup>§</sup> Ref. 26

<sup>¶</sup> Ref. 21

<sup>||</sup> Ref. 28

stants,  $e_{ij}$ ,<sup>33</sup> we compute the clamped-ion component and the Born effective charges using the self-consistent response to an applied electric field. The ionic contribution to the piezoelectric tensor is calculated from finite differences. Elastic constants, also required to compute piezoelectric polarization, are similarly calculated from finite differences.

### 3 Results

#### 3.1 Band alignments

##### 3.1.1 Band structure

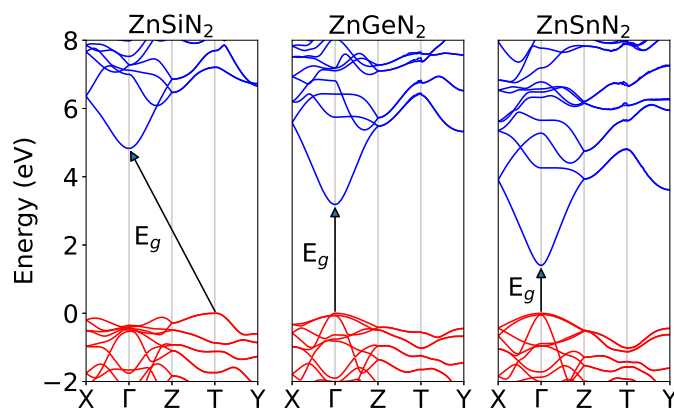


Fig. 2 Calculated band structures of the Zn-IV-nitrides.

In Fig. 2, we illustrate the band structures of the Zn-IV-nitrides. In all three materials, the VBM is primarily composed of N  $p$  states, while the conduction-band minimum (CBM) has mostly  $s$  character. The band gaps of ZnSnN<sub>2</sub> and ZnGeN<sub>2</sub> are direct at the  $\Gamma$  point, while the band gap of ZnSiN<sub>2</sub> is indirect with the VBM at T and the CBM at  $\Gamma$ . Band gaps are listed in Table 1.

##### 3.1.2 Surface calculations

In Table 2, we list the VBM and CBM with respect to the vacuum level as obtained from surface calculations in which the atomic positions are not relaxed; effects of atomic relaxation are discussed below. Conduction-band positions for the III-nitrides are obtained based on  $E_{\text{VBM}}$  and the experimental band gaps. These results allow us to determine the band alignments shown in Fig. 3. The band offsets between the three Zn-IV-nitrides are “type I”, i.e., the band edges of the material with the smaller gap lie within the band gap of the material with the larger gap, similar to how the III-nitrides are aligned. Between ZnGeN<sub>2</sub> and GaN, there is a type-II alignment: the VBM and CBM of ZnGeN<sub>2</sub> are both lower in energy than the corresponding bands in GaN.

We investigated atomic relaxations and found them to have only a small effect on alignments. Allowing the atoms in the slab to relax resulted in a lowering of the average electrostatic potential within the slab by 0.1–0.2 eV for all three Zn-IV-nitrides. We also examined alignments based on slabs with a different orientation, namely (010), a nonpolar surface analogous to (11 $\bar{2}$ 0) ( $a$  plane) in the III-nitrides. For this surface orientation the average electrostatic potential in the slab is systematically slightly higher (by up to 0.14 eV) than for the (100) surface. Relaxation of the

atoms for the (010) surface results in a larger shift of the electrostatic potential than for (100): a lowering by  $0.30 \pm 0.05$  eV is found for each of the Zn-IV-nitrides. These effects are consistent with the  $0.30 \pm 0.01$  eV reduction in the electrostatic potential upon relaxation for GaN and InN surfaces found by Moses *et al.*<sup>19</sup> The differences are systematic, and as a result very similar band alignments are obtained irrespective of whether relaxed or non-relaxed surfaces are used in the calculations.

##### 3.1.3 Hydrogen alignment

Calculation of the  $H_i(+/-)$  transition level provides an alternative approach method to align band structures.<sup>20</sup> We calculate the  $H_i(+/-)$  levels relative to the VBM, and in Table 2 and Fig. 3 we combine this information with the positions of the valence-band edges obtained from surface calculations. Among the Zn-IV-nitrides, the position of the  $H_i(+/-)$  level varies by only 0.1 eV on an absolute energy scale, showing that alignment based on the  $H_i(+/-)$  level is very consistent with the alignment based on surface calculations.

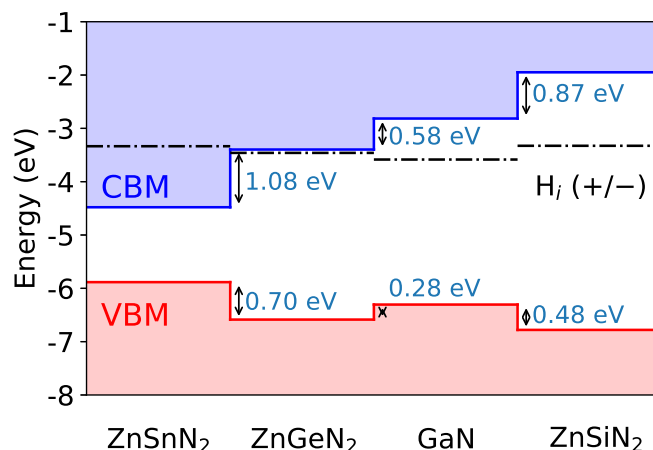


Fig. 3 Band alignments between Zn-IV-nitrides and GaN, shown on an absolute energy scale where zero is the vacuum level.

##### 3.1.4 Comparison with previous calculations

The band alignment between ZnSnN<sub>2</sub> and GaN has been calculated by two other groups, using a superlattice geometry: Wang *et al.*<sup>14</sup> found a VB offset of  $-0.39$  eV, while Punya *et al.*<sup>12,13</sup> calculated a VB offset of  $-1.4$  eV. Our calculated offset of  $-0.42$  eV is very close to the value reported by Wang *et al.*, but disagrees with the Punya *et al.* result by 1.0 eV. Punya *et al.* also reported the VBM of ZnGeN<sub>2</sub> to be 1.1 eV higher than that of GaN, while we find the VBM of ZnGeN<sub>2</sub> to be 0.28 eV lower than that of GaN: a difference of 1.4 eV.

The difference with the results of Punya *et al.* is likely due to the difference in computational approach. While we (and Wang *et al.*<sup>14</sup>) use the HSE functional, Punya *et al.* used the LDA functional and applied a correction based on  $GW$  calculations. It is known that  $GW$  results can depend on the accuracy of the DFT calculations used as a starting point.

Based on superlattice calculations for cubic ZnGeN<sub>2</sub>/GaN Cao *et al.*<sup>17</sup> found a VB offset of  $-0.38$  eV, a difference of 0.70 eV from

Table 2 Position of the valence-band maximum  $E_{\text{VBM}}$  and conduction-band minimum  $E_{\text{CBM}}$  with respect to the vacuum level as obtained from surface calculations for nonpolar (100) Zn-IV-nitride and  $(\bar{1}\bar{1}00)$  GaN surfaces. InN and AlN values are from Ref. 19. The  $H_i(+/-)$  was calculated relative to the VBM and then combined with the  $E_{\text{VBM}}$  values to obtain a position relative to the vacuum level. All values are in eV.

	ZnSnN <sub>2</sub>	ZnGeN <sub>2</sub>	ZnSiN <sub>2</sub>	InN	GaN	AlN
$E_{\text{CBM}}$	-4.48	-3.40	-1.95	-5.04	-2.82	-0.60
$E_{\text{VBM}}$	-5.88	-6.59	-6.78	-5.69	-6.30	-6.76
$H_i(+/-)$	-3.33	-3.46	-3.34	...	-3.58	...

our results. The discrepancy here is likely due to the fact they are evaluating the (001) interface for cubic material, i.e., a different interface and crystal structure from what we evaluate here.

## 3.2 Polarization

### 3.2.1 Spontaneous polarization

The Zn-IV-nitrides have an orthorhombic unit cell, with space group  $Pna2_1$  and point group  $mm2$ .  $Pna2_1$  is a polar space group that has two glide planes, and as such it has two nonpolar axes and one polar axis. The direction along the polar axis is labeled the  $c$  direction, consistent with the notation for the wz III-nitrides. We calculate the spontaneous polarization along this polar axis.

As explained in Sec. 2.3, the effective spontaneous polarization is the difference between the formal polarization of the orthorhombic structure and the formal polarization of a reference structure, for which we choose the centrosymmetric  $Pnma$  structure. Because formal polarization is multivalued, we need to ensure that we compare the same branch of the polarization for both structures. This is accomplished by calculating the formal polarization of structures interpolated between the end points such that the differences in formal polarization are significantly smaller than the quantum of polarization  $\frac{e\hbar}{\Omega}$ . The spontaneous polarization as a function of interpolated atomic coordinates is shown in Fig. 4. Inserts show the unit cells for the orthorhombic  $Pna2_1$  structure and the centrosymmetric  $Pnma$  structure of ZnGeN<sub>2</sub>. The effective spontaneous polarization values for the Zn-IV-nitrides are listed in Table 3.

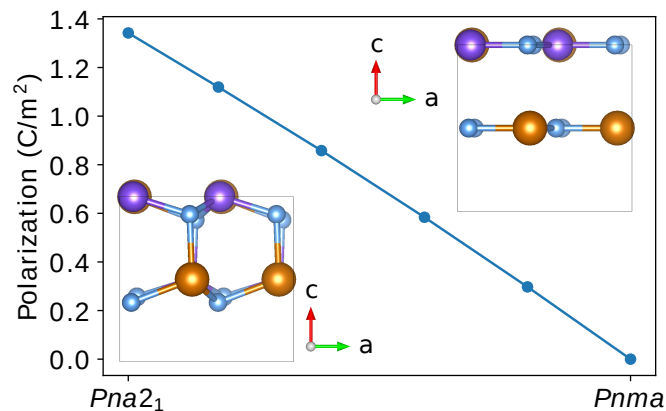


Fig. 4 Spontaneous polarization as a function of interpolated atomic coordinates between the orthorhombic  $Pna2_1$  structure and the high-symmetry  $Pnma$  structure of ZnGeN<sub>2</sub>.

In Fig. 5, we plot the spontaneous polarization for the III-nitrides and the Zn-IV-nitrides as a function of lattice param-

eter. For the Zn-IV-nitrides, we use  $a_{\text{wz}} = \sqrt{\frac{ab}{2\sqrt{3}}}$  to define a wurtzite-equivalent lattice parameter. To determine the spontaneous polarization of alloys, we first convert to the reduced units of  $\frac{e\hbar}{\Omega} = e/A_{\text{int}}$  (the quantum of polarization), where  $A_{\text{int}} = \sqrt{3}a_{\text{wz}}^2$  is the area of the base of the wz unit cell [drawn in Fig. 1(a)]. In these units, we interpolate the spontaneous polarization linearly, then convert back to  $\text{Cm}^{-2}$ . This method accounts for the areal dependence of the polarization.

	ZnSnN <sub>2</sub>	ZnGeN <sub>2</sub>	ZnSiN <sub>2</sub>
$P_{\text{SP}}$	1.184	1.333	1.433
$P_{\text{SP}}$ (zb ref)	-0.033	-0.027	-0.029
$P_{\text{SP}}$ (zb ref), Ref. 4	-0.029	-0.023	-0.022

eter. For the Zn-IV-nitrides, we use  $a_{\text{wz}} = \sqrt{\frac{ab}{2\sqrt{3}}}$  to define a wurtzite-equivalent lattice parameter. To determine the spontaneous polarization of alloys, we first convert to the reduced units of  $\frac{e\hbar}{\Omega} = e/A_{\text{int}}$  (the quantum of polarization), where  $A_{\text{int}} = \sqrt{3}a_{\text{wz}}^2$  is the area of the base of the wz unit cell [drawn in Fig. 1(a)]. In these units, we interpolate the spontaneous polarization linearly, then convert back to  $\text{Cm}^{-2}$ . This method accounts for the areal dependence of the polarization.

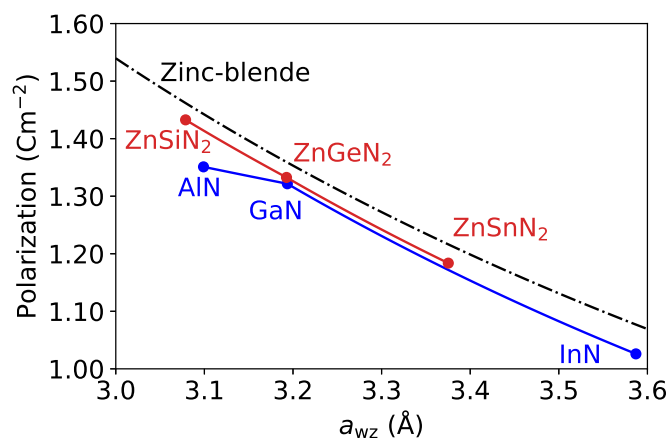


Fig. 5 Spontaneous polarization for the III-nitrides and the Zn-IV-nitrides, as a function of wurtzite-equivalent in-plane lattice parameter  $a_{\text{wz}}$ . The values for a zinc-blende structure are also indicated.

Our calculations indicate that the spontaneous polarization values of ZnGeN<sub>2</sub> and GaN are quite similar. More generally, the spontaneous polarization of ZnSnGeN<sub>2</sub> alloys and InGaN alloys is very similar at the same lattice parameter. Interestingly, there is a significant spontaneous polarization difference between ZnSiGeN<sub>2</sub> and AlGaIn.

Paudel *et al.*<sup>4</sup> previously calculated spontaneous polarization constants for the Zn-IV-nitrides, reporting values in the narrow range of  $-0.022 \text{ Cm}^{-2}$  to  $-0.029 \text{ Cm}^{-2}$ . However, they used a zb structure as their reference. In Fig. 5 we also show the formal polarization (along the [111] axis) for a zb structure. For zb, the

magnitude of the appropriate branch of the formal polarization is  $P_f^{zb} = e\sqrt{3}/2a_{wz}^2$  (see Ref. 21), which is equivalent to  $\frac{3e}{4A_{int}}$ ; i.e., the value for zb depends only on the lattice parameter. This allows us to express our spontaneous polarization values with respect to a zb reference; the values are shown in Table 3, and compared to the values reported in Ref. 4. Reasonable agreement is found.

We caution against using spontaneous polarization values referenced to zb. Each material has different lattice parameters for the zb reference structure, which leads to additional terms in polarization differences calculated at an interface (due to the fact that the formal polarization of zb is nonzero).<sup>21</sup> Those terms have not been properly included in conventional simulations. When the centrosymmetric structures (which have zero formal polarization) are used as the reference, additional terms are not necessary.

### 3.2.2 Piezoelectric polarization

For piezoelectric polarization, there are five nonzero piezoelectric tensor elements for orthorhombic materials with the *mm2* point group.<sup>34</sup> We calculate the proper piezoelectric coefficients,  $e_{ij} = \frac{dJ_i}{d\epsilon_j}$ , where  $J_i$  is the current density that flows through the bulk of the material in response to a strain  $d\epsilon_j$ . For purposes of calculating polarization differences at pseudomorphic interfaces between two semiconductors, *improper* piezoelectric coefficients should be used.<sup>21,33</sup> Here we calculate the proper piezoelectric coefficients because they are branch-independent and can be compared to experimental values.<sup>33</sup> Improper coefficients are related to the proper coefficients by expressions that involve the zero-strain (spontaneous) formal polarization.<sup>21,33</sup> The improper piezoelectric constants  $e_{31}$  and  $e_{32}$  are related to the respective proper constants by

$$e_{3i}^{imp} = e_{3i}^{prop} - P_{SP}, \quad (1)$$

while the improper coefficient  $e_{33}^{imp}$  is the same as the proper coefficient. Our calculated proper piezoelectric constants are listed in Table 4. The values of  $e_{31}$  and  $e_{32}$  are close to the values of  $e_{31}$  in the III-nitrides, while the values of  $e_{33}$  are significantly smaller than the values of  $e_{33}$  for the III-nitrides.<sup>21</sup>

Table 4 Calculated proper piezoelectric polarization constants for the Zn-IV-nitrides. All values in  $\text{Cm}^{-2}$ .

	ZnSnN <sub>2</sub>	ZnGeN <sub>2</sub>	ZnSiN <sub>2</sub>
$e_{15}$	-0.307	-0.302	-0.279
$e_{24}$	-0.286	-0.262	-0.241
$e_{31}$	-0.397	-0.378	-0.386
$e_{32}$	-0.403	-0.299	-0.305
$e_{33}$	0.825	0.666	0.692

Elastic constants are also required to calculate piezoelectric polarization at pseudomorphic interfaces. Calculated elastic constants are listed in Table 5. The values are in good agreement with previously published calculations.<sup>4</sup>

### 3.2.3 Polarization charges at interfaces

Polarization differences between materials manifest in interface charges at a heterojunction. For an interface normal to the *c* axis

Table 5 Calculated elastic constants of the Zn-IV-nitrides. All values in GPa.

	ZnSnN <sub>2</sub>	ZnGeN <sub>2</sub>	ZnSiN <sub>2</sub>
$C_{11}$	270	342	403
$C_{22}$	255	330	372
$C_{33}$	285	385	467
$C_{23}$	91	103	119
$C_{13}$	93	98	101
$C_{12}$	115	138	150
$C_{44}$	67	97	124
$C_{55}$	63	87	104
$C_{66}$	73	108	138

the interface charge  $\sigma_b$  can be calculated based on the polarization properties and the elastic constants<sup>21</sup>:

$$\sigma_b = P_{SP}^m - P_{SP}^n - \sum_{i=1,2} \epsilon_i^n (e_{3i}^n - P_{SP}^n - e_{33}^n C_{i3}^n / C_{33}^n). \quad (2)$$

Here we assume that material *n* is strained coherently to material *m* (i.e., *m* is the substrate, or a layer much thicker than *n*) and grown along the +*c* axis. We will denote such an interface as *n/m*.  $P_{SP}$  is the spontaneous polarization,  $\epsilon_i$  are the strain components,  $e_{ij}$  are the piezoelectric coefficients, and  $C_{ij}$  are the elastic constants. Parameters for AlN and InN were taken from Ref. 21. Elastic parameters for the III-nitrides have been taken from Ref. [28].

Unlike the III-nitrides, the Zn-IV-nitrides exhibit an anisotropy in lattice parameters perpendicular to the *c* axis (see Table 1). A ZnGeN<sub>2</sub> layer strained to a *c*-plane GaN substrate experiences a tensile strain  $\epsilon_1$  in the [100] direction, but compressive strain  $\epsilon_2$  in the [010] direction. The in-plane lattice parameters can be visually compared in Fig. 1(c). The strain  $\epsilon_3$  in the direction normal to the interface can be calculated using the elastic constants (Table 5). Each of these strains  $\epsilon_j$  produces a piezoelectric effect along the *c* direction with coefficient  $e_{3j}$ .

In Fig. 6, we plot the total (spontaneous + piezoelectric) polarization for Zn-IV-nitrides strained to wz substrates with a given lattice parameter  $a_{wz}$ . Units of  $e/A_{int}$  are chosen for clarity of visualization, since the polarization differences are more difficult to discern when expressed in units of  $\text{Cm}^{-2}$  (as evident from Fig. 5). The total polarization lines extend up to  $\pm 2\%$  average planar strain (note that the strains along *a* and *b* axes are different; this anisotropy is taken into account in the calculation of the piezoelectric polarization). The dashed lines in Fig. 6 correspond to strained material. The differences between the total polarization of the strained Zn-IV-nitrides (black dashed lines) and the spontaneous polarization values for the III-nitride alloys (solid cyan line) at the same lattice parameter are precisely the bound charges at an interface between the two materials, in accordance with Eq. (2). Similarly, differences between the total polarization of the strained III-nitrides (pink dashed lines centered at AlN and GaN) and spontaneous polarization values for the Zn-IV-nitrides correspond precisely to the bound charges at the interface between AlN or GaN strained to ZnSi<sub>x</sub>Ge<sub>1-x</sub>N<sub>2</sub> or ZnGe<sub>x</sub>Sn<sub>1-x</sub>N<sub>2</sub> at a given wurtzite-equivalent lattice parameter  $a_{wz}$ .

For ZnGeN<sub>2</sub> strained to GaN the total polarization difference

is  $0.0052 e/A_{\text{int}}$  or  $5.9 \times 10^{12} e/\text{cm}^2$ . This interface exhibits a very small net piezoelectric effect, as  $\text{ZnGeN}_2$  strained to GaN is slightly tensile strained along the  $a$  axis, and slightly compressed along the  $b$  axis. As result, the total polarization difference is primarily a result of the difference in the spontaneous polarization values. Similarly, the differences in polarization values between the strained III-nitrides (purple lines) and unstrained II-IV-nitrides (red line) correspond to bound charges at an interface between the two materials. To identify an interface with zero polarization difference, we would look for a point where the blue and green lines intersect; this happens, e.g., for an interface between strained  $\text{ZnGeN}_2$  and  $\text{In}_{0.09}\text{Ga}_{0.91}\text{N}$ .

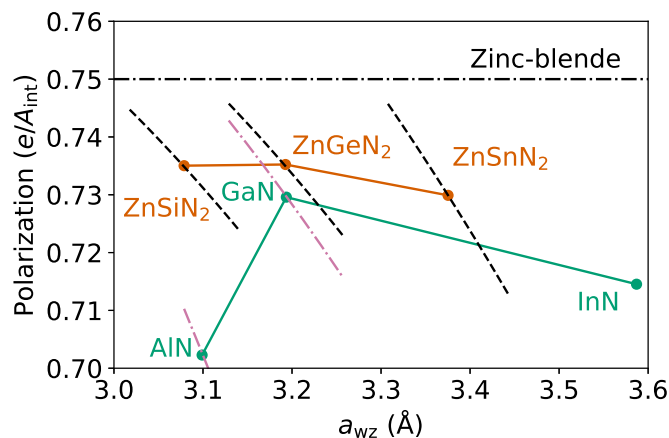


Fig. 6 Solid lines indicate the interpolated spontaneous polarization for Zn-IV-nitride alloys and III-nitride alloys. These are plotted as a function of the in-plane wurtzite lattice parameter (where we use a wurtzite-equivalent lattice parameter for the Zn-IV-nitrides). For each of the Zn-IV-nitrides, black dashed lines indicate the total polarization (spontaneous + piezoelectric) assuming the material is strained to a III-nitride alloy substrate with the wurtzite lattice parameter on the horizontal axis. For each of the III-nitrides, pink dash-dotted lines indicate the total polarization assuming the material is strained to a Zn-IV-nitride alloy substrate with a given wurtzite-equivalent lattice parameter on the horizontal axis.

The anisotropic in-plane strain at the  $\text{ZnGeN}_2/\text{GaN}$  interface distinguishes it from conventional III-nitride interfaces. The average wurtzite-equivalent in-plane lattice parameter of  $\text{ZnGeN}_2$  is very close to that of GaN, and the piezoelectric polarization from the strain along the  $a$  axis mostly cancels the effect along the  $b$  axis. This cancellation leaves the spontaneous polarization as the primary contribution to the interface charge at the interface. This is in contrast to III-nitride interfaces, where the piezoelectric effect dominates over the spontaneous polarization. Piezoelectric contributions will also be important for interfaces with other Zn-IV-nitrides, which do not exhibit a close (average) lattice match.

## 4 Prospects for polarization engineering with Zn-IV-nitrides

### 4.1 Light emitters

We now examine, based on our calculated values of band alignments and polarization constants, specific structures which could improve the light-emission efficiency of nitride quantum wells.

The cases discussed here are only examples of the rich space that is opened up by integrating the Zn-IV-nitrides with III-nitrides.  $c$ -plane devices lead to strong polarization fields, which separate electrons and holes in the quantum well and reduce radiative recombination. To overcome the Stark effect, the use of nonpolar or semipolar orientations has been proposed,<sup>35,36</sup> but growth in those orientations tends to be harder to control than for the  $c$  plane.

An alternative approach is the use of  $c$ -plane heterostructures with interfaces that minimize the polarization charge. In Fig. 6, we showed that a  $\text{ZnGeN}_2$  layer strained to  $\text{In}_{0.09}\text{Ga}_{0.91}\text{N}$  results in an interface with zero polarization charge. The choice of substrate has only a minor effect on the required composition to achieve zero polarization charge: a  $\text{ZnGeN}_2/\text{In}_{0.07}\text{Ga}_{0.93}\text{N}$  interface strained to GaN would also have zero polarization charge. These zero-polarization charge structures are not possible within the InGaN ternary system alone; to achieve zero- (or reduced-) polarization structures within the III-nitrides system requires using nonpolar or semipolar orientations, or quaternary alloys.

Minimizing polarization fields is only one aspect of enhancing light emission; the heterostructure also needs to provide adequate confinement for electrons and holes in a quantum well. In Fig. 7, we plot the band offsets between  $\text{ZnGeN}_2$  and ternary III-nitrides; a positive value indicates the band edge of the III-nitride is higher in energy than that of  $\text{ZnGeN}_2$ . For concentrations of In lower than 24%, the CB of InGaN is above the CB of  $\text{ZnGeN}_2$ , indicating that there will be no quantum confinement for electrons in the InGaN quantum well. This means that the heterostructure with zero polarization charge (with < 24% In) cannot be directly used for a quantum well device. Electron confinement would require In concentration higher than 24%.

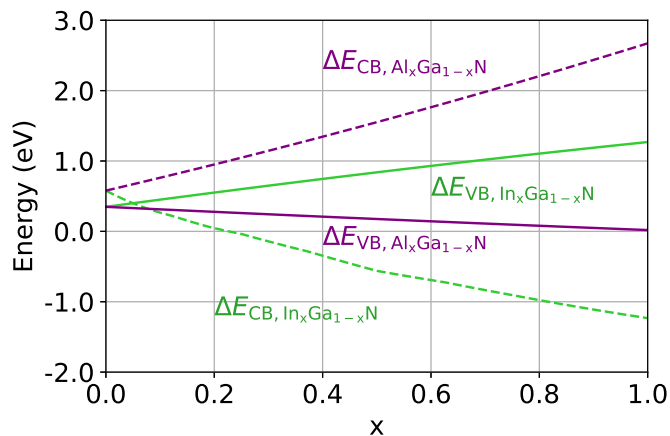


Fig. 7 CB and VB offsets for AlGaN and InGaN layers relative to the CBM and VBM of  $\text{ZnGeN}_2$ . Band bowing parameters for InGaN are from Ref. 19 and for AlGaN from Ref. 37. Strain effects are taken into account using deformation potentials from Refs. 38 and 39.

Finally, we comment on proposals for optoelectronic device structures incorporating Zn-IV-nitrides in InGaN quantum wells.<sup>6,7,40</sup> The aim was to counteract the Stark effect by confining holes in a thin  $\text{ZnGeN}_2$  layer. Such confinement of holes will occur only if the  $\text{ZnGeN}_2$  valence band lies above the VBM in

the III-nitride alloy. The simulations of Ref. 6, 7, and 40 relied on the values calculated by Punya *et al.*<sup>12,13</sup>, which show a large and negative value for the ZnGeN<sub>2</sub>/GaN VB offset (−1.1 eV). As discussed in Sec. 3.1.4, our present calculations show that this is not the case; i.e., we find the ZnGeN<sub>2</sub>/GaN VB offset to be positive. Therefore the Zn-IV-nitride layer is not able to confine holes, thus casting doubt on these predictions.

## 4.2 Transistors

For electronic applications, enhanced interfacial polarization charge can be beneficial since it allows achieving higher carrier densities.<sup>3</sup> If ZnSiN<sub>2</sub> can be grown with sufficiently high quality, forming heterostructures with AlGaN could be advantageous both for electron confinement and for enhanced polarization. Our calculations indicate that the CBM of ZnSiN<sub>2</sub> is 1.6 eV below that of AlN, while the VBM of ZnSiN<sub>2</sub> is only slightly lower than that of AlN. The large CB offset is beneficial for the two-dimensional electron gas at a ZnSiN<sub>2</sub> strained-to-AlN interface. We find the polarization charge to be  $-3.5 \times 10^{13} \text{ cm}^{-2}$  at the ZnSiN<sub>2</sub>/AlN interface, which is comparable to an interface between GaN and Al<sub>0.5</sub>Ga<sub>0.5</sub>N. This high polarization charge and large band offset makes ZnSiN<sub>2</sub> an interesting material for electronic applications.

## 5 Conclusions

We have performed a comprehensive study of band alignments and polarization properties of heterostructures between the Zn-IV-nitrides and the III-nitrides. Values for spontaneous and piezoelectric polarization coefficients are reported. We have demonstrated that the Zn-IV-nitrides allow for new combinations of polarization and band gap, which might enable novel device structures. We have identified zero-polarization-charge interfaces between Zn-IV-nitrides and III-nitrides; however these structures cannot be used for quantum-well devices due to the band offsets. Heterostructures between GaN and ZnGeN<sub>2</sub> exhibit a type-II offset, in which the valence band of ZnGeN<sub>2</sub> is lower than in GaN. For electronic devices, ZnSiN<sub>2</sub>/AlN interfaces exhibit a larger conduction-band offset than AlGaN/GaN, along with a large polarization charge, thus allowing for potentially higher electron sheet densities. The cases discussed are only examples of the rich space that is opened up by integrating the Zn-IV-nitrides with III-nitrides; the parameters reported in this paper will enable the exploration of this space.

## Conflicts of interest

There are no conflicts to declare.

## Acknowledgements

We thank C. E. Dreyer for helpful discussions about determining spontaneous polarization. This work was supported by the Army Research Office (W911NF-16-1-0538). Work by DW on ZnGeN<sub>2</sub> was supported by the US Department of Energy (DOE), Office of Science, Basic Energy Sciences (BES) under Award No. DE-SC0010689 and work by DW on ZnSiN<sub>2</sub> and ZnSnN<sub>2</sub> was supported by a National Research Council Fellowship at the US Naval Research Laboratory. Computational resources were provided by

the Department of Defense High Performance Computing Modernization Program at the Army Research Office/Office of Naval Research (Project No. ARONC4175) and by the Extreme Science and Engineering Discovery Environment (XSEDE) (supported by National Science Foundation (NSF) grant number ACI-1548562). We also used computational facilities purchased with funds from NSF (CNS-1725797) and administered by the Center for Scientific Computing (CSC). The CSC is supported by the California NanoSystems Institute and the Materials Research Science and Engineering Center (MRSEC; NSF DMR 1720256) at UC Santa Barbara.

## References

- 1 P. C. Quayle, K. He, J. Shan and K. Kash, *MRS Commun.*, 2013, **3**, 135–138.
- 2 A. D. Martinez, A. N. Fioretti, E. S. Toberer and A. C. Tamboli, *J. Mater. Chem. A*, 2017, 11418–11435.
- 3 O. Ambacher, J. Smart, J. R. Shealy, N. G. Weimann, K. Chu, M. Murphy, W. J. Schaff, L. F. Eastman, R. Dimitrov, L. Wittmer, M. Stutzmann, W. Rieger and J. Hilsenbeck, *J. Appl. Phys.*, 1999, **85**, 3222–3233.
- 4 T. R. Paudel and W. R. L. Lambrecht, *Phys. Rev. B*, 2009, **79**, 245205.
- 5 L. Han, C. Lieberman and H. Zhao, *J. Appl. Phys.*, 2017, **121**, 093101.
- 6 L. Han, K. Kash and H. Zhao, *J. Appl. Phys.*, 2016, **120**, 103102.
- 7 B. Hyot, M. Rollès and P. Miska, *physica status solidi (RRL) – Rapid Research Letters*, 2019, **13**, 1900170.
- 8 M. F. Schubert, J. Xu, J. K. Kim, E. F. Schubert, M. H. Kim, S. Yoon, S. M. Lee, C. Sone, T. Sakong and Y. Park, *Appl. Phys. Lett.*, 2008, **93**, 041102.
- 9 S. F. Chichibu, A. C. Abare, M. S. Minsky, S. Keller, S. B. Fleischer, J. E. Bowers, E. Hu, U. K. Mishra, L. A. Coldren, S. P. DenBaars and T. Sota, *Appl. Phys. Lett.*, 1998, **73**, 2006–2008.
- 10 U. K. Mishra, P. Parikh and Y.-F. Wu, *Proc. IEEE*, 2002, **90**, 1022–1031.
- 11 D. Jena, J. Simon, A. Wang, Y. Cao, K. Goodman, J. Verma, S. Ganguly, G. Li, K. Karda, V. Protasenko, C. Lian, T. Kosel, P. Fay and H. Xing, *Phys. Status Solidi A*, 2011, **208**, 1511–1516.
- 12 A. Punya and W. R. L. Lambrecht, *Phys. Rev. B*, 2013, **88**, 075302.
- 13 A. P. Jaroenjittichai, S. Lyu and W. R. L. Lambrecht, *Phys. Rev. B*, 2017, **96**, 079907.
- 14 T. Wang, C. Ni and A. Janotti, *Phys. Rev. B*, 2017, **95**, 205205.
- 15 J. Heyd, G. E. Scuseria and M. Ernzerhof, *J. Chem. Phys.*, 2006, **124**, 219906.
- 16 J. Heyd, G. E. Scuseria and M. Ernzerhof, *J. Chem. Phys.*, 2003, **118**, 8207.
- 17 R. Cao, H.-X. Deng, J.-W. Luo and S.-H. Wei, *J. Semiconductors*, 2019, **40**, 042102.
- 18 P. Narang, S. Chen, N. C. Coronel, S. Gul, J. Yano, L.-W. Wang, N. S. Lewis and H. A. Atwater, *Adv. Mater.*, 2014, **26**, 1235–

- 1241.
- 19 P. G. Moses, M. Miao, Q. Yan and C. G. Van de Walle, *J. Chem. Phys.*, 2011, **134**, 084703.
- 20 C. G. Van de Walle and J. Neugebauer, *Nature*, 2003, **423**, 626.
- 21 C. E. Dreyer, A. Janotti, C. G. Van de Walle and D. Vanderbilt, *Phys. Rev. X*, 2016, **6**, 021038.
- 22 G. Kresse and J. Hafner, *Phys. Rev. B*, 1993, **47**, 558–561.
- 23 G. Kresse and J. Furthmüller, *Comput. Mater. Sci.*, 1996, **6**, 15–50.
- 24 P. Blöchl, *Phys. Rev. B*, 1994, **50**, 17953.
- 25 M. Wintenberger, M. Maunay and Y. Laurent, *Mater. Res. Bull.*, 1973, **8**, 1049 – 1053.
- 26 H. Jonas, S. Saskia, W. Peter and S. Wolfgang, *Chem. Eur. J*, 2017, **23**, 12275–12282.
- 27 A. Baldereschi, S. Baroni and R. Resta, *Phys. Rev. Lett.*, 1988, **61**, 734–737.
- 28 I. Vurgaftman and J. R. Meyer, *J. Appl. Phys.*, 2003, **94**, 3675–3696.
- 29 C. Freysoldt, B. Grabowski, T. Hickel, J. Neugebauer, G. Kresse, A. Janotti and C. G. Van de Walle, *Rev. Mod. Phys.*, 2014, **86**, 253–305.
- 30 R. D. King-Smith and D. Vanderbilt, *Phys. Rev. B*, 1993, **47**, 1651–1654.
- 31 D. Vanderbilt and R. D. King-Smith, *Phys. Rev. B*, 1993, **48**, 4442–4455.
- 32 R. Resta and D. Vanderbilt, in *Theory of Polarization: A Modern Approach*, Springer Berlin Heidelberg, Berlin, Heidelberg, 2007, pp. 31–68.
- 33 D. Vanderbilt, *Journal of Physics and Chemistry of Solids*, 2000, **61**, 147 – 151.
- 34 J. Nye, *Physical Properties of Crystals: Their Representation by Tensors and Matrices*, Clarendon Press, 1985.
- 35 M. C. Schmidt, K.-C. Kim, R. M. Farrell, D. F. Feezell, D. A. Cohen, M. Saito, K. Fujito, J. S. Speck, S. P. DenBaars and S. Nakamura, 2007, **46**, L190–L191.
- 36 D. F. Feezell, M. C. Schmidt, S. P. DenBaars and S. Nakamura, *MRS Bulletin*, 2009, **34**, 318–323.
- 37 A. Kyrtsos, M. Matsubara and E. Bellotti, *Phys. Rev. B*, 2019, **99**, 035201.
- 38 A. Janotti and C. G. Van de Walle, *Phys. Rev. B*, 2007, **75**, 121201.
- 39 Q. Yan, P. Rinke, M. Winkelkemper, A. Qteish, D. Bimberg, M. Scheffler and C. G. Van de Walle, *Semicond. Sci. Tech.*, 2010, **26**, 014037.
- 40 H. Fu, J. C. Goodrich, O. Ogidi-Ekoko and N. Tansu, *J. Appl. Phys.*, 2019, **126**, 133103.

- A table of contents entry: graphic maximum size 8 cm x 4 cm and one sentence of text, maximum 20 words, highlighting the novelty of the work

Calculations of band alignments and polarization properties of the Zn-IV-nitrides highlight the promise of these materials for wide-band gap electronics.

